Journal of Materials Chemistry

Cite this: J. Mater. Chem., 2012, 22, 2057

www.rsc.org/materials

PAPER

Electrically conductive and high temperature resistant superhydrophobic composite films from colloidal graphite†

I. S. Bayer,*[ab] V. Caramia,[a] D. Fragouli,[a] F. Spano,[a] R. Cingolani[c] and A. Athanassiou*[ac]

Received 27th September 2011, Accepted 10th November 2011
DOI: 10.1039/c1jm14813c

Electrically conductive and self-cleaning superhydrophobic films (water contact angles >160°, droplet roll off angles <5°) were fabricated by simply solution casting sub-micron polytetrafluoroethylene (Teflon) particle dispersed alcohol-based colloidal graphite solutions. The process is very suitable for forming conductive superhydrophobic coatings on glasses, metals, ceramics and high performance polymers such as polyimide (Kapton®). The solutions were deposited on microscope glass slides and Kapton® films by drop casting. After solvent evaporation under ambient conditions, the coatings were annealed to melt Teflon. Upon melting, Teflon particles fused into one another forming a hydrophobic polymer matrix. The degree of superhydrophobicity and the surface morphology of the coatings together with their electrical conductivity were studied in detail by varying Teflon-to-graphite weight fractions. A number of applications can be envisioned for these coatings such as electrode materials for energy conversion devices, high performance electromagnetic shielding materials, flexible electronic components and heat exchanger surfaces, to name a few.

Introduction

The term colloidal graphite is very commonly used in the electronics industry and refers to high concentration (20 wt%) solid suspensions of submicron graphite particles in a carrier liquid, generally water or alcohol.[1] Colloidal graphite is often used for making conductive electrical connections or electrodes for energy conversion devices[2–5] and also for lubricating surfaces.[6] In nuclear power plants, for instance, conductive colloidal graphite is used in large quantities as an anti-seize compound, thread lubricant and for lubricating moving parts and rubbing surfaces. It has also been tested as an electromagnetic shielding admixture into cement.[7] A very recent study successfully demonstrated the use of colloidal graphite as a conducting and catalytic counter-electrode for dye synthesized solar cells.[8] Colloidal graphite has also been utilized for the efficient detection of lipids, proteins and peptides with laser desorption/ionization mass spectrometry.[9] Commercially available water suspensions of graphite are usually stabilized with small amounts of tannic acid or ammonia and alcohol suspensions usually contain less than 5 wt% cellulose acetate,[6] which enables continuous conductive film formation. In general, conducting dry films obtained from commercial colloidal graphite solutions, containing approximately 20 wt% solids, display 40 Ω μm^{-1} sheet resistance.[10]

Fabrication of superhydrophobic materials with additional functionality such as electrical conductivity, magnetism, light emission, antimicrobial activity, *etc.* has been gaining rapid academic and industrial interest, as an increasing number of simple, inexpensive, and durable superhydrophobic materials have been demonstrated.[11–16] Recently, a series of conducting superhydrophobic films have been reported by dispersing nanostructured conductive fillers in hydrophobic polymer matrices.[17,18] Such electrically conductive superhydrophobic films can be used as non-wetting electromagnetic interference (EMI) shielding materials,[19] as smart textiles,[15,20,21] in "lab on a chip" applications, and in printing electronics.[22] Detailed electrical characterization of superhydrophobic systems is important in order to identify the type of conductivity such as ohmic or diode-like as well as breakdown voltages if superhydrophobic materials are to be integrated into various devices. In general, most studies report sheet resistance in terms of Ω sq^{-1} or conductivity in terms of S m^{-1}.[18,23–27] Resistance of conducting superhydrophobic materials against peel off, mechanical abrasion, solvent etching and elevated temperatures is also of great importance and needs to be improved.[28]

In this study, we demonstrate a simple and inexpensive procedure to fabricate highly conductive superhydrophobic films from alcohol-based colloidal graphite, by blending colloidal graphite with submicron polytetrafluoroethylene (Teflon) dispersed isopropyl alcohol solutions. Teflon–graphite composite films can be made by simply drop casting from blended solutions. In particular, the technique is very suitable to

[a]*Center for Biomolecular Nanotechnologies@UNILE, Istituto Italiano di Tecnologia, Via Barsanti, Arnesano, LE, 73010, Italy. E-mail: ilker.bayer@iit.it; athanassia.athanassiou@iit.it*
[b]*Department of Mechanical and Aerospace Engineering, University of Virginia, Charlottesville, 22904, USA*
[c]*Istituto Italiano di Tecnologia, Via Morego 30, Genova, 16163, Italy*
† Electronic supplementary information (ESI) available. See DOI: 10.1039/c1jm14813c

form conducting superhydrophobic films on glass, ceramic, metal, and high temperature resistant polymers such as polyimide (Kapton®) films. Wetting of the composites as a function of Teflon-to-graphite weight fraction was characterized by measuring static water contact angles and droplet roll off angles (the tilt angle of the substrate at which water droplets freely roll off the surfaces). The electrical conductivity of the films was characterized by measuring current–voltage curves (biased between −20 V and +20 V) using a semiconductor parameter analyzer. Surface topology of the films was studied with an atomic force microscope (AFM) in non-contact mode.

Experimental

Isopropanol based colloidal graphite was purchased from TAAB Laboratories, UK. Its overall solids content is made up of 20 wt % graphite particles (400–900 nm in size) and of less than 5 wt% cellulose acetate as a film forming agent. Sub-micron Teflon powder was purchased from Sigma-Aldrich. The average Teflon particle size is approximately 200 nm.[13] Various concentrations of Teflon powder were dispersed in reagent grade isopropanol using a standard ultrasonic processor for 10 to 15 minutes. No dispersant or surfactants were used. It was found that the maximum amount of Teflon that can be suspended in isopropanol was 10 wt% above which significant gelation of the suspension occurred. The concentration of the as received colloidal graphite was reduced by dilution with isopropanol so that stock solutions of colloidal graphite from 1 wt% up to 15 wt% can be prepared.

Diluted colloidal graphite solutions were sonicated for an additional $^1/_2$ hour. Following this, Teflon solutions were blended into the graphite solutions during continuous sonication from which different composite films containing varying Teflon-to-graphite weight fractions were cast. The blends were drop cast on hydrophilic microscope glass slides and Kapton® films and were allowed to dry overnight under ambient conditions. Typical film thickness was of the order of 20 μm. The substrates were then transferred onto a hotplate maintained at 350 °C and annealed for $^1/_2$ min to allow melting of Teflon particles. Note that the melting temperature of Teflon is 325 °C. Annealed films were cooled to room temperature gradually. In order to test the high temperature resistance of the fabricated films, some samples were kept on a hotplate maintained at 500 °C continuously for 4 h and after cooling to room temperature additional contact angle measurements were taken.

Surface morphology and roughness of the composite films were analyzed by an atomic force microscope (AFM), Park Systems XE-100, in non-contact mode using a silicon cantilever. An adaptive scan rate set between 0.15 Hz and 0.25 Hz was utilized for all samples. Electrical characteristics of the composites were measured using an Agilent 4155B Semiconductor Analyzer interfaced with a Karl Suss RA150 Probe Station. Samples were biased from −20 V to +20 V and current–voltage (I–V) data were recorded at 0.1 V intervals. Conductive silver paste electrodes were painted on sample surfaces in order to minimize the contact resistance. The gap between the painted silver electrodes was 1 mm. Minimum five I–V measurements were taken from each sample at different time intervals in order to assess the electrical stability and repeatability of the measurements.

Wetting characteristics of the films were measured by distilled water droplets using a contact angle goniometer manufactured by Kruss, Germany. Droplet roll off angles were determined on a homemade tilt stage which could be mounted to the contact angle goniometer setup. Various ethanol–water mixtures were prepared in order to construct Zisman plots to estimate the surface energy of the superhydrophobic films. In particular, six different ethanol–water mixtures were prepared: 5%, 10%, 25%, 40%, 50% and 80% by weight with corresponding surface tensions of 56.4, 48.1, 36.1, 30.7, 28.5 and 24.3 mN m^{-1}. The surface tension values of ethanol–water mixtures were obtained from ref. 29. Three to five contact angle measurements were taken from each liquid within ±3° uncertainty.

Results and discussions

Before blending Teflon suspensions with colloidal graphite, the morphological and wetting characteristics of Teflon films obtained by drop casting from their isopropanol suspensions were investigated. Fig. 1(a) shows the topographical AFM image of a film obtained by drop casting from a 3 wt% Teflon suspension in isopropanol. The film is formed by densely packed sub-micron Teflon particles. In Fig. 1(b) the shape of the Teflon particles is shown in more detail. Their shape in general appears to be of an elongated sphere form. Surprisingly, when this film was annealed (melted) at 350 °C, the morphology transforms into a fibrillar network as shown in Fig. 1(c).

When the submicron particles melt, they appear to fuse into one another forming elongated fibrillar networks, which randomly organize into larger domains as shown in Fig. 1(c). Fig. 2 shows the 3D topology of the films shown in Fig. 1(a) and (c) and the corresponding static water contact angle and droplet roll off angle measurements conducted on both films. Here, we present measurements taken from 20 different drop-cast films prepared from the same isopropanol suspension in order to analyze the reproducibility of the wetting characteristics. Static water contact angles on the films before annealing reached 157° on average and droplet roll off angles were below 10° as seen in Fig. 2. Static water contact angles on the annealed films however declined to 140° on average, while droplet roll off angles increased to 45°. This can possibly be attributed to the disappearance of the surface roughness due to closely packed Teflon particles upon melting. Indeed, in general, static water contact angles measured on smooth Teflon surfaces range from 120° to 140° depending on the roughness and history of the Teflon surface.[30]

Similarly, morphology and wetting characteristics of graphite films were analyzed by AFM and contact angle measurements. Fig. 3(a) shows the AFM non-contact mode topographical image of a graphite film obtained by drop casting as-received colloidal graphite on a glass slide after sonication for 15 minutes. The image indicates that the colloidal graphite is made up of graphite particles of various sizes and shapes ranging from sub-micron to micron. The apparent morphology seen in Fig. 3(a) is typical of graphitic solid lubricant films composed of layered planar structures which can easily shear to provide low friction.[6] The arrows in Fig. 3(a) show the exposed edges of some graphene

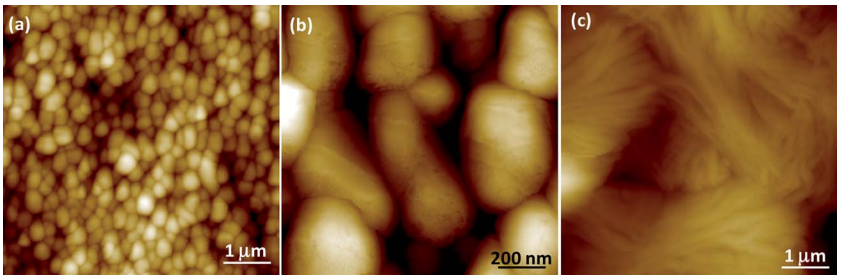

Fig. 1 (a) AFM topography acquired in non-contact mode of a Teflon film obtained by drop casting 3 wt% Teflon suspensions in isopropanol. (b) A smaller area scan of the film shown in (a), showing the geometrical shape of the sub-micron Teflon particles. (c) AFM topography of the film in (a), after thermal annealing at 350 °C for 30 s. Annealing-induced morphological change into a fibrillar network is clearly seen.

platelets forming the planar layered structures. Fig. 3(b) shows the scanning electron microscope (SEM) image of a fractured surface of the same film after partially washing away cellulose acetate, preexisting in the colloidal graphite solution, with acetone. This was done by immersing the film in acetone for some time to dissolve the cellulose acetate partially. Morphological details of graphite particles with various sizes and shapes are more evident in this image. Drop cast films from as received colloidal graphite were of hydrophilic nature with an average water static contact angle of 63°. No droplets could roll off the surfaces even if substrate tilt angles exceeded 90°.

Superhydrophobic films could be formed only when certain Teflon to graphite mass fractions were maintained in the composite films. The most promising composites displaying self-cleaning superhydrophobicity were observed in dry films having 1.2 to 2.2 Teflon-to-graphite weight fractions as a result of thermal annealing. After solvent evaporation, dry films, before annealing at 350 °C to melt Teflon, showed a mixed degree of hydrophobicity with high contact angle hysteresis depending on the Teflon-to-graphite weight fraction. In addition, before annealing, the films had very poor substrate adhesion for both glass and Kapton® and could be easily removed from the substrates by gentle rubbing. Therefore, annealing to melt Teflon

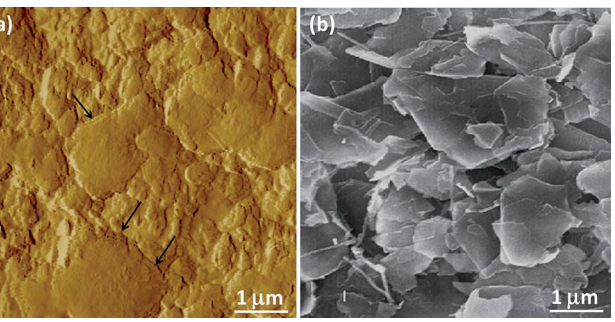

Fig. 3 (a) An AFM topographical image of an as received colloidal graphite film drop cast on a glass slide. Arrows indicate exposed edges of graphene planes. (b) A scanning electron microscope image of a fractured surface of the film after partially washing away trace amounts of cellulose acetate originating from colloidal graphite by acetone.

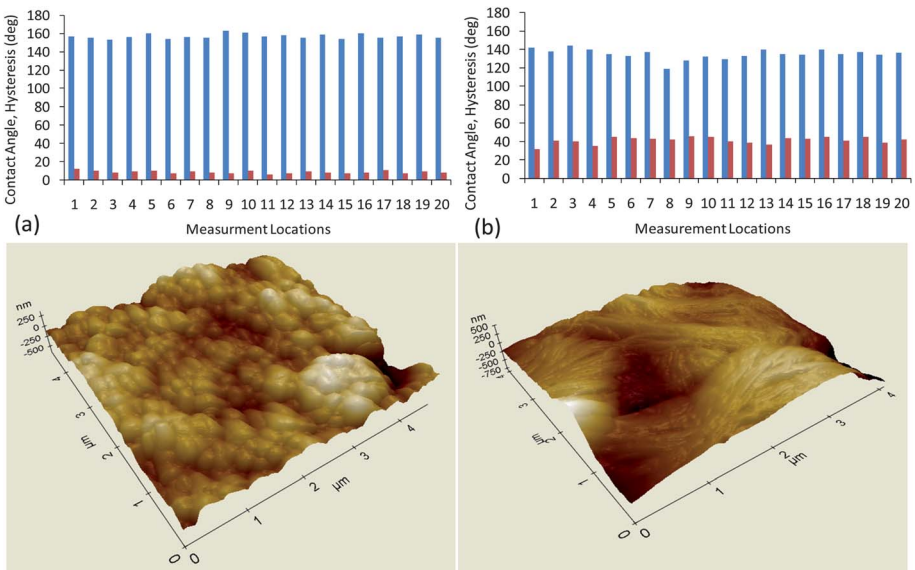

Fig. 2 (a) Top: static water contact angle and water droplet roll off angle measurements taken from 20 different films, and their indicative 3D topography (bottom). (b) Top: static water contact angle and water droplet roll off angle measurements and a 3D topography image of the above-mentioned films after thermal annealing (bottom). In the top graphs, blue bars denote static contact angle data and red bars denote contact angle hysteresis.

served two purposes: (a) melting induced generation of self-cleaning superhydrophobicity and (b) formation of a good degree of substrate adhesion. Fig. 4(a) shows a photograph of a microscope glass slide coated with a superhydrophobic film having a Teflon-to-graphite mass fraction of 2.2 after annealing for $^1/_2$ min. The sessile water droplet contact angle on this surface was 167°. In Fig. 4(b) the photograph of the same film deposited on a piece of Kapton® film is shown.

Fig. 5(a) shows the AFM topography of the same composite film shown in Fig. 4(a) and in Fig. 5(b) a 3D surface roughness topology is presented. The roughness appears to be made up of sharp randomly oriented pyramid-like features with an average roughness value of approximately 600 nm. Comparison of Fig. 3 (a) and 5(a) indicates that when Teflon melts in the presence of graphite, the graphite particles get reoriented and their edges appear to be protruding from the surface in a random way. Such polymer melting-induced surface structuring is considered to be responsible for the occurrence of self-cleaning super-hydrophobicity by enhancing the surface roughness. Polymer melting-induced surface morphology changes can be observed more clearly in the phase contrast AFM images of the composites before and after Teflon melting which will be discussed in relation to Fig. 8.

The wetting of the annealed films was analyzed by measuring sessile water droplet contact angles and droplet roll off angles as a function of Teflon-to-graphite weight fraction. In addition, by using various ethanol–water mixtures as probe liquids within a surface tension range of 22 mN m^{-1} to 72 mN m^{-1} the surface energy of the superhydrophobic composites was estimated by constructing Zisman plots.[31,32] The surface tension of ethanol–water mixtures was obtained from Vazquez *et al.*[29] Zisman plots are constructed by measuring contact angles of various liquids having a wide range of surface tensions and plotting the cosine of the measured contact angle (cos θ) *versus* liquid surface tension for each liquid used provided that the selected liquids would not chemically interact with the surface. The data should cluster around a linear trend and can be fitted with a line. Interpolating the fitted line to cos $\theta = 1$ yields an estimated surface energy for the surface under question.[32,33] Fig. 6(a) shows a plot of the sessile water droplet contact angle *versus* Teflon-to-graphite weight fraction as well as water droplet roll off angles measured on all annealed films. As seen in the graph, films with a Teflon-to-graphite weight fraction of 1.2 and above are all super-hydrophobic. However, for the films with Teflon-to-graphite weight fractions of 1 and 1.2, droplet roll off angles are somewhat greater than 10°. Fig. 6(b) shows Zisman plots for three different films with the corresponding Teflon-to-graphite weight fraction of 1.2, 1.5 and 2.2, respectively. From the data in this figure it is seen that the surface energy of all the films is practically the same even though the Teflon-to-graphite weight fraction was almost doubled from 1.2 to 2.2.

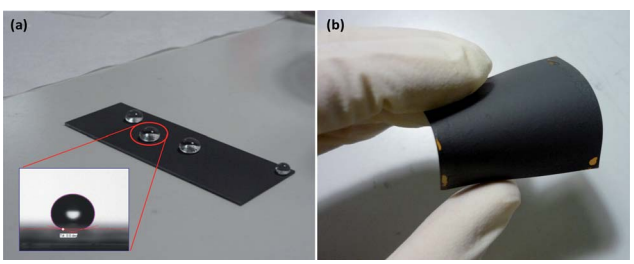

Fig. 4 (a) Photograph of a microscope glass slide coated with a conducting superhydrophobic film with a Teflon-to-graphite weight fraction of 2.2. Sessile water droplet contact angle on this film is 167°. (b) Photograph of a Kapton® film coated with the same conductive super-hydrophobic composite. Both films were annealed at 350 °C for $^1/_2$ min.

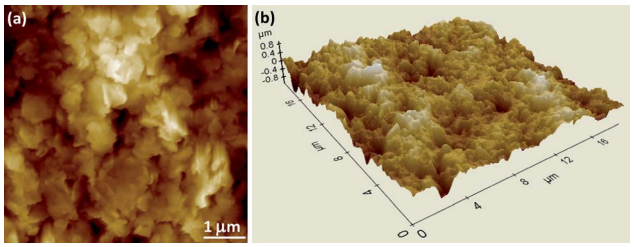

Fig. 5 (a) AFM topographical image of a superhydrophobic film drop cast on a microscope glass slide and annealed with a Teflon-to-graphite weight fraction of 2.2. (b) A 3D scan of the same film showing surface roughness features due to graphite rearrangement during polymer melting.

All the films studied did not display any low surface tension liquid (solvent) repellency against liquids such as alcohols, and hydrocarbon liquids like hexane, which have liquid surface tensions below 30 mN m^{-1}. This is attributed to the fact that polytetrafluoroethylene (Teflon, a linear fluoro-resin) has no higher perfluoro side chains compared to perfluoroacrylic copolymers for instance[34] and hence Teflon is an oleo- and solvent-philic polymer. Finally, all the five superhydrophobic annealed films shown in Fig. 6 were kept at 500 °C for four hours continuously and no degradation in superhydrophobicity was measured. This is expected since both Teflon and Kapton® films do not thermally degrade before 600 °C.[35]

Next, we investigated electrical conductivity of the composite films deposited on microscope glass slides before annealing, as a function of Teflon-to-graphite weight fraction. Five different films were biased from −20 V to +20 V at 0.1 V intervals. Linear (ohmic) *I–V* curves were obtained (Fig. 7) for all the composites having 1, 1.2, 1.5, 1.8 and 2.2 Teflon-to-graphite weight fractions. Each *I–V* curve shown in Fig. 7 is the average of five measurements taken at different times from each film. The inset table in Fig. 7 shows the calculated conductivity of each film as a function of Teflon-to-graphite weight fraction. Electrical conductivity of the films is of the order of 10^3 S m^{-1}, which is two orders of magnitude less than the conductivity of pure graphite, but an order of magnitude higher than recently reported conducting super-hydrophobic surfaces containing carbon nanofibers, which were designed for terahertz frequency shielding applications.[19] The electrical conductivity values of these composites are among the few highest reported so far in the literature.[23,26,36] It is important to note that composites with higher conductivity than the ones reported in Fig. 7 were also fabricated by decreasing the Teflon-to-graphite weight fraction but at the expense of reduced static water contact angles (<150°) and highly increased contact angle hysteresis. Therefore, such data were not reported herein since the composites were not of self-cleaning superhydrophobic nature. However, compared to other conductive superhydrophobic polymer nanocomposites,[23] the present composites display very high self-cleaning water contact angles when the polymer to filler

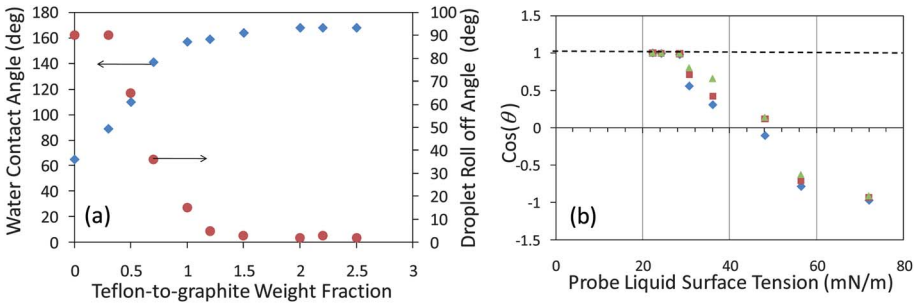

Fig. 6 (a) Sessile water contact angle and droplet roll off angle as a function of the Teflon-to-graphite ratio. (b) Zisman plots for three different films with Teflon-to-graphite weight fractions of 1.2 (diamonds), 1.5 (squares) and 2.2 (triangles). Estimated surface energies corresponding to each weight fraction are 21 mJ m^{-2}, 24 mJ m^{-2} and 27 mJ m^{-2}, respectively. The uncertainty in surface energy estimation is within 5 mJ m^{-2}.

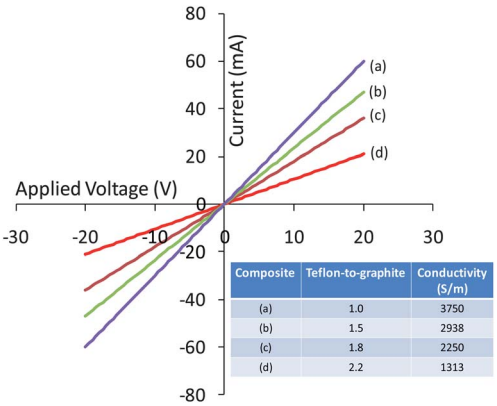

Composite	Teflon-to-graphite	Conductivity (S/m)
(a)	1.0	3750
(b)	1.5	2938
(c)	1.8	2250
(d)	2.2	1313

Fig. 7 *I–V* plots for five different conducting superhydrophobic films deposited on microscope glass slides with Teflon-to-graphite weight fractions of 1, 1.2, 1.5, 1.8 and 2.2 corresponding to labels (a), (b), (c) and (d), respectively. The inset table shows the electrical conductivity of the superhydrophobic films as a function of Teflon-to-graphite weight fraction.

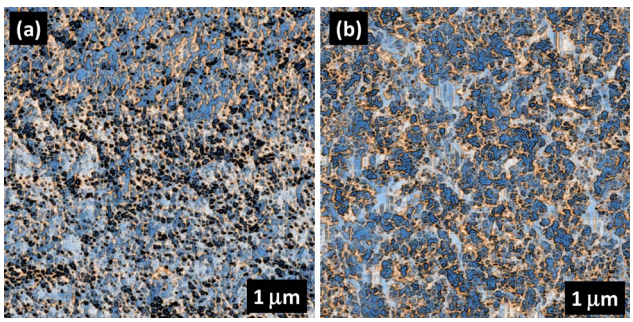

Fig. 8 (a) Color enhanced AFM phase contrast image of a conducting composite film before annealing to melt Teflon and (b) AFM phase contrast image of the conducting superhydrophobic film obtained after annealing the film in (a), at 350 °C for $^1/_2$ min. The film has a Teflon-to-graphite weight fraction of 2.2.

ratio reaches 1 whereas for superhydrophobicity in some carbon nanotube–polymer (Nafion) composites this ratio was reported to be 0.1.[23] This means that less functional filler is required to obtain similar electrical conductivity while maintaining extreme water repellency.

Electrical conductivity of the films before and after annealing to melt Teflon was on average the same; hence the process of converting the films into the superhydrophobic state by melting Teflon did not cause any degradation in electrical conductivity. To this end, we have collected several phase contrast images using AFM from these films before and after annealing to qualitatively assess this observation. Fig. 8(a) shows a phase contrast image of a film corresponding to a Teflon-to-graphite weight fraction of 2.2 before annealing to melt Teflon. Phase contrast image data collected from nanostructured polymer composites are in general quite difficult to interpret. In particular, for polymeric materials the phase signal is sensitive to the degree of crystallinity, viscoelastic properties and adhesion forces.[31] This is because the phase is really a measure of the energy dissipation involved in the contact between the tip and the sample, which depends on a number of factors, including such features as viscoelasticity, adhesion and also contact area. As contact area is dependent on the slope of the sample, the phase image also contains topographic contributions. Therefore, in these cases, understanding the contribution of the individual factors to the phase shift is not simple. Despite the complications involved in interpretation, phase contrast is one of the most commonly used techniques for phase continuity and composition characterization of such sample surfaces. Dark blue regions or spots which are seen in Fig. 8(a) correspond to individual Teflon particles which are somewhat dispersed throughout the surface of the film. The white regions represent exposed graphite particles on the surface whereas light blue regions could be due to surface structures corresponding to highly aggregated Teflon particles. The yellowish thin regions, on the other hand, correspond to the exposed edges of the graphite platelets. When Teflon melts as a result of annealing (Fig. 8(b)) it appears to be distributed throughout the surfaces as a polymer matrix indicated by further expansion of the blue regions over the surface. The white regions are probably the exposed graphite particles on the surface. A noticeable difference (increase) in the distribution and intensity of the yellowish thin regions has appeared in this image which can be due to the polymer melt induced orientation of graphite platelets in such a way that more graphite platelet edges protrude from the surface.

These protruding edges in Fig. 8(b) are well connected and form an interpenetrating structure within the Teflon matrix compared to the structure shown in Fig. 8(a). As mentioned earlier, the electrical conductivity of the composite thin films before and after annealing was practically the same; however melting Teflon enabled the films to adhere to the substrates and prevented them from dissolving in liquids when dipped.

Considering a number of potential applications of these thin film composites such as electrode materials for energy conversion devices or heat exchanger surfaces where liquid condensation takes place, structural and electrical stability of these films in electrolytic media becomes crucial. Therefore the process of annealing improves substrate adhesion (both glass and Kapton®) at the same time maintaining their conductive properties. Although the data in Fig. 6(b) revealed that the surface energy of all the annealed superhydrophobic composite films, for the Teflon-to-graphite weight fraction ranging from 1.2 to 2.2, is practically the same, their conductivity changes significantly when the Teflon-to-graphite weight fraction is doubled, as seen in Fig. 7. This might enable one to design superhydrophobic composite films with tunable electrical conductivity without sacrificing self-cleaning superhydrophobicity.

Conclusions

A simple and inexpensive technique was described to fabricate electrically conductive and high temperature resistant superhydrophobic films from submicron Teflon dispersed commercial alcohol-based colloidal graphite. The films were obtained simply by drop casting on microscope glass slides and Kapton® films. The films were annealed at 350 °C for $^1/_2$ minute so that Teflon particles were melted forming a continuous polymeric matrix. The surface topology of the films was inspected with non-contact AFM measurements. The films displayed very stable ohmic behavior when biased between −20 V and +20 V. The wetting characteristics of the films were analyzed by measuring sessile water droplet contact angles and droplet roll off angles as a function of Teflon-to-graphite weight fraction. The surface energy of the superhydrophobic films was also estimated using contact angle measurements from various ethanol–water mixtures. It was found that the surface energy of all the superhydrophobic films was practically the same even though the Teflon-to-graphite weight fraction was almost doubled from 1.2 to 2.2. However, the conductivity of the superhydrophobic surfaces decreased significantly when the Teflon-to-graphite weight fraction was doubled. These composite coatings can find various applications such as electrode materials for batteries, high performance electromagnetic shielding materials, flexible electronic components and heat exchanger surfaces, to name a few.

References

1 S. B. Bibikov, V. N. Gorshenev, R. S. Sharafiev and A. M. Kuznetsov, *Mater. Chem. Phys.*, 2008, **108**, 39–44.
2 J. Wu and D. D. L. Chung, *J. Electron. Mater.*, 2005, **34**, 1255–1258.
3 J. Cao and D. D. L. Chung, *Carbon*, 2003, **41**, 1309–1328.
4 J.-M. Kauffmann, A. Laudet, G.-J. Patriarche and G. D. Christian, *Talanta*, 1982, **29**, 1077–1082.
5 J. Ping, J. Wu and Y. Ying, *Electrochem. Commun.*, 2010, **12**, 1738–1741.
6 P. J. Martorana, I. S. Bayer, A. Steele and E. Loth, *Ind. Eng. Chem. Res.*, 2010, **49**, 11363–11368.
7 J. Cao and D. D. L. Chung, *Cem. Concr. Res.*, 2003, **33**, 1737–1740.
8 G. Veerappan, K. Bojan and S.-W. Rhee, *ACS Appl. Mater. Interfaces*, 2011, **3**, 857–862.
9 S. Cha and E. S. Yeung, *Anal. Chem.*, 2007, **79**, 2373–2385.
10 C. E. Thorn, F. Polakovic and C. A. Mosolf, *US Pat.*, 5476580, 1995.
11 I. S. Bayer, A. Brown, A. Steele and E. Loth, *Appl. Phys. Express*, 2009, **2**, 125003–125006.
12 T. Verho, C. Bower, P. Andrew, S. Franssila, O. Ikkala and R. H. A. Ras, *Adv. Mater.*, 2011, **23**, 673–678.
13 M. K. Tiwari, I. S. Bayer, G. M. Jursich, T. M. Schutzius and C. M. Megaridis, *ACS Appl. Mater. Interfaces*, 2010, **2**, 1114–1119.
14 I. S. Bayer, A. Steele, P. J. Martorana and E. Loth, *Appl. Phys. Lett.*, 2009, **94**, 163902–163905.
15 I. S. Bayer, A. Biswas and G. Ellialtioglu, *Polymer Compos.*, 2011, **32**, 576–585.
16 T. M. Schutzius, M. K. Tiwari, I. S. Bayer and C. M Megaridis, *Composites, Part A*, 2011, **42**, 979–985.
17 S. Sethi and A. Dhinojwala, *Langmuir*, 2009, **25**, 4311–4313.
18 M. Peng, Z. Liao, J. Qi and Z. Zhou, *Langmuir*, 2010, **26**, 13572–13578.
19 A. Das, C. M. Megaridis, L. Liu, T. Wang and A. Biswas, *Appl. Phys. Lett.*, 2011, **98**, 174101–174103.
20 H. Wang, Y. Xue and T. Lin, *Soft Matter*, 2011, **7**, 8158–8161.
21 Y. Zhu, J. Li, H. He, M. Wan and L. Jiang, *Macromol. Rapid Commun.*, 2007, **28**, 2230–2236.
22 D. Barona and A. Amirfazli, *Lab Chip*, 2011, **11**, 936–940.
23 C. Luo, X. Zuo, L. Wang, E. Wang, S. Song, J. Wang, J. Wang, C. Fan and Y. Cao, *Nano Lett.*, 2008, **8**, 4454–4458.
24 M. Sansotera, W. Navarrini, G. Resnati, P. Metrangolo, A. Famulari, C. L. Bianchi and P. A. Guarda, *Carbon*, 2010, **48**, 4382–4390.
25 M. Peng, J. Qi, Z. Zhou, Z. Liao, Z. Zhu and H. Guo, *Langmuir*, 2010, **26**, 13062–13064.
26 M. Fang, Z. Tang, H. Lu and S. Nutt, *J. Mater. Chem.*, 2012, **22**, 109–114.
27 J. T. Han, S. Y. Kim, J. S. Woo and G.-W. Lee, *Adv. Mater.*, 2008, **20**, 3724–3727.
28 Y. Zhu, J. C. Zhang, J. Zhai, Y. M. Zheng, L. Feng and L. Jiang, *ChemPhysChem*, 2006, **7**, 336–341.
29 G. Vazquez, E. Alvarez and J. M. Navaza, *J. Chem. Eng. Data*, 1995, **40**, 611–614.
30 J.-B. Donet and R.-Y. Qin, *J. Colloid Interface Sci.*, 1992, **154**, 434–443.
31 K. D. O'Neil and O. A. Semenikhin, *J. Phys. Chem. C*, 2007, **111**, 14823–14832.
32 Y. Kano and S. Akiyama, *Polymer*, 1992, **33**, 1690–1695.
33 I. S. Bayer, C. M. Megaridis, J. Zhang, D. Gamota and A. Biswas, *J. Adhesion Sci. Technol.*, 2007, **21**, 1439–1467.
34 A. Steele, I. Bayer and E. Loth, *Nano Lett.*, 2009, **9**, 501–505.
35 K. A. Klinedinst, W. M. Vogel and P. Stonehart, *J. Mater. Sci.*, 1976, **11**, 794–800.
36 T. M. Schutzius, I. S. Bayer, M. K. Tiwari and C. M. Megaridis, *Ind. Eng. Chem. Res.*, 2011, **50**, 11117–11123.

